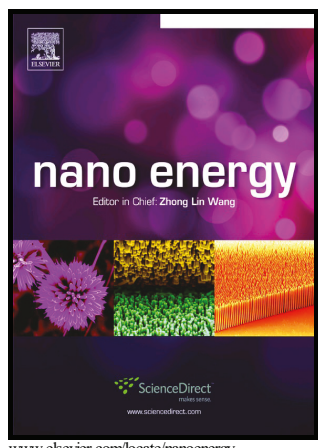
# Author's Accepted Manuscript

High-Frequency Electrochemical Capacitors Based on Plasma Pyrolyzed Bacterial Cellulose Aerogel for Current Ripple Filtering and Pulse Energy Storage

Nazifah Islam, Shiqi Li, Guofeng Ren, Yujiao Zuo, Juliusz Warzywoda, Shu Wang, Zhaoyang Fan



www.elsevier.com/locate/nanoenergy

PII: S2211-2855(17)30485-8

http://dx.doi.org/10.1016/j.nanoen.2017.08.015 DOI:

NANOEN2129 Reference:

To appear in: Nano Energy

Received date: 20 July 2017 9 August 2017 Revised date: Accepted date: 10 August 2017

Cite this article as: Nazifah Islam, Shiqi Li, Guofeng Ren, Yujiao Zuo, Juliusz Warzywoda, Shu Wang and Zhaoyang Fan, High-Frequency Electrochemical Capacitors Based on Plasma Pyrolyzed Bacterial Cellulose Aerogel for Current Ripple Filtering and Pulse Storage, Nano Energy Energy, http://dx.doi.org/10.1016/j.nanoen.2017.08.015

This is a PDF file of an unedited manuscript that has been accepted for publication. As a service to our customers we are providing this early version of the manuscript. The manuscript will undergo copyediting, typesetting, and review of the resulting galley proof before it is published in its final citable form. Please note that during the production process errors may be discovered which could affect the content, and all legal disclaimers that apply to the journal pertain.

# CCEPTED MANUSCR

High-Frequency Electrochemical Capacitors Based on Plasma Pyrolyzed Bacterial Cellulose

Aerogel for Current Ripple Filtering and Pulse Energy Storage

Nazifah Islam<sup>1</sup>, Shiqi Li<sup>1</sup>, Guofeng Ren<sup>1</sup>, Yujiao Zuo<sup>2</sup>, Juliusz Warzywoda<sup>3</sup>, Shu Wang<sup>2</sup>, Zhaoyang Fan<sup>1</sup>\*

<sup>1</sup>Department of Electrical and Computer Engineering and Nano Tech Center, Texas Tech University,

Lubbock, TX 79409, USA

<sup>2</sup>Department of Nutritional Sciences, Texas Tech University, Lubbock, TX 79409, USA

<sup>3</sup>Materials Characterization Center, Whitacre College of Engineering, Texas Tech University, Lubbock,

TX 79409, USA

\*Email: Zhaoyang.Fan@ttu.edu

Keywords: High-frequency supercapacitor; kilohertz supercapacitor; electrochemical capacitor; AC

filtering; pulse energy storage; plasma pyrolysis

**Abstract** 

There are great needs in developing compact-size kilohertz (kHz) high-frequency (HF) electrochemical

capacitors (ECs) for ripple current filtering and environmental vibration energy harvesting. However, the

previously demonstrated electrodes are generally limited to a very small areal capacitance density at 120

Hz due to sub-um thick electrode used for meeting frequency requirement, which renders them unsuitable

for practical ECs. Here, using crosslinked carbon nanofiber aerogel, derived from rapid microwave

plasma pyrolysis of bacterial cellulose that was synthesized in a fermentation process, we demonstrated

kHz HF-ECs with areal capacitance density as high as 4.5 mF cm<sup>-2</sup> at 120 Hz in an aqueous electrolyte.

The cruciality of plasma pyrolysis on high frequency response of the derived carbon nanofiber aerogel

was discussed. The electrode performance in an organic electrolyte was further studied for operation in a

large potential window of more than 3 V. Using such kHz HF-ECs, we further demonstrated their

applications in rapid pulse energy storage for vibrational energy harvesting, as well as in ripple current

filtering for AC/DC conversion. The promising results suggest this technology has great potential for

1

developing practical compact HF-ECs in substitution of electrolytic capacitors for several crucial applications.

#### Introduction

Electrochemical capacitors (ECs) are being widely investigated to increase their energy density, to function as independent energy source or in supplement with the low power batteries. As energy sources, ECs have a charge and discharge rate (frequency) limited up to approximately 1 s (1 Hz). In other words, they work under direct current (DC). They will behave more like a resistor but not a capacitor at higher frequencies. Therefore, these conventional ECs cannot play the roles of conventional electrolytic capacitors that work at much higher frequencies for ripple current filtering, <sup>1-2</sup> decoupling, high-frequency pulse energy storage, and other functions.

A huge performance gap exists between conventional ECs and electrolytic capacitors.<sup>3</sup> ECs provide much larger capacitance density than electrolytic capacitors, but the latter can respond at tens of kilohertz (kHz) frequencies. Since electrolytic capacitors are commonly used for ripple current filtering in AC/DC converters and DC links, while their large size is becoming a limiting factor in downscaling the circuit design, there are great needs and interests in developing high-frequency (HF) ECs for filtering applications. For 60 Hz line-frequency, considering the harmonic frequencies after rectification, such HF-ECs should respond at hundreds to kilo hertz range. In another frontier, environmental energy harvesting through piezoelectric- or triboelectric-generator is promising for self-powered autonomous sensors and internet of things (IOT) technology, while the environmental mechanical energy sources and hence the outputs from the micro-generators are typically pulsed currents with tens or hundreds Hz.<sup>4-6</sup> They also require kHz HF-ECs to efficiently store the harvested energy.

To evaluate the response frequency of a capacitor, the characteristic frequency  $f_0$  when the impedance phase angle reaches  $-45^{\circ}$  is commonly used, which defines the boundary between capacitance dominance and resistance dominance. Of the two categories of ECs, pseudocapacitors are intrinsically slow even though fast pseudocapacitors were reported,  $^{7-8}$  while electric double layer capacitors (EDLCs)

in principle are capable of charging and discharging within milliseconds, promising for kHz HF-ECs. <sup>9-13</sup> This strongly depends on the nanostructure of electrodes, conductivity of the electrode material and the choice of electrolyte. <sup>3, 14</sup> In terms of the electrode nanostructure, reduction of porosity and electrode thickness <sup>15-16</sup> to accelerate electrolyte ions transport is the key for high-frequency response. However, this diminishes the achievable capacitance.

Towards high-frequency response<sup>3</sup> by partially sacrificing capacitance, vertically-oriented graphene (VOG)<sup>1, 9, 13</sup> and carbon nanotube (CNT) ultra-thin film<sup>11, 17</sup> have been widely studied. Since very thin (~ 1 μm to 0.1 μm) "active" materials were used, they provided a very limited areal capacitance density. For conventional sandwich-type cell configuration, practical consideration requires a fairly thick active material layer to minimize the mass and volume penalties associated with the inactive components that include separators, electrolytes, current collectors, and packaging. This is particularly true when multiple cells have to be serially packed together for a high voltage rating. This films or 3D structures, including reduced graphene oxide (rGO) aerogel,<sup>2</sup> carbon black/VOG, <sup>18</sup> edge-oriented graphene (EOG),<sup>10, 12</sup> holey rGO film,<sup>19</sup> CMK3/CNT composite,<sup>20</sup> and others<sup>21</sup> were therefore reported with larger areal capacitance density. Further improving the areal capacitance to a new level is in demand for compact HF-ECs. In addition, most demonstrations are based on aqueous electrolytes due to their high ionic conductivity. However, with a limited potential window (< 1 V), aqueous electrolyte restricts the volumetric capacitance density in a high-voltage EC since more units are required to be connected in series to obtain a given rating voltage. In this regard, an organic electrolyte with potential window up to ~ 3 V has its merit.<sup>20, 22-23</sup>

Here we report crosslinked carbon nanofiber aerogel derived from pyrolysis of bacterial cellulose (BC) cultivated using Kombucha strains, as freestanding electrodes for kHz HF-ECs with much larger areal capacitance density. The whole process is illustrated in Figure 1a. The carbonized BC (CBC) aerogel electrode was produced by pyrolysis of BC aerogel in microwave plasma of hydrogen and methane (CH<sub>4</sub>) mixture for only 15 minutes. The pyrolyzed product, with a suitable porous structure, was directly applied as electrodes to assemble coin cells without any further processing. Compared to other

reports involving complex steps in preparation of nanostructured electrode,  $^{24\cdot27}$  the fabrication route adopted here is simple and straightforward, and the produced CBC electrodes were demonstrated to be very suitable for HF-ECs. In particular, CBC electrodes in an aqueous electrolyte exhibited  $f_0 = 3.3$  kHz and  $C_A^{120} = 2.98$  mF cm<sup>-2</sup> or  $f_0 = 1.3$  kHz and  $C_A^{120} = 4.50$  mF cm<sup>-2</sup> for two different thickness, where  $f_0$  is the characteristic frequency when the phase reaches  $-45^\circ$  and  $C_A^{120}$  is the areal capacitance density at 120 Hz. Our results are extraordinary considering that most publications report a limited  $C_A^{120}$  values, resulting in a packaged HF-EC without significant preponderance in term of volumetric density when comparing to electrolytic capacitors.<sup>3</sup> The pyrolysis conditions on high frequency response of the CBC aerogel was discussed. It deserves to emphasize that pyrolyzed bacterial cellulose through thermal process was reported previously as electrodes for ECs.<sup>25, 28-32</sup> However, those ECs are still conventional slow ECs due to a different pyrolysis process used, as will be discussed by comparing the different pyrolysis processes. The operating voltage range of our CBC based HF-ECs was further expanded to 3 V by utilizing an organic electrolyte for practical applications. With the assembled HF-ECs, their applications for ripple current filtering and pulse energy harvesting and storage were further demonstrated.

#### **Results and discussion**

#### **BC** and **CBC** material studies

Carbon nanostructures derived from natural biomass are being studied as renewable resources for electrode applications. Cellulose microfibrils secreted by bacteria are of particular appeal.<sup>33-34</sup> They are long hydrocarbon polymer chains with a diameter of 1.78 nm, which form 3-4 nm bundles through hydrogen bonding, and then into nanoribbons, and further crosslink into a three-dimensional web structure.<sup>35</sup>

In our study, BC pellicles were produced in a fermentation process using Kombucha strains, <sup>36</sup> the method used for production of Kombucha tea, as detailed in the Supplemental Information (SI). One BC pellicle cultivated in a container is shown in Figure S1a in the SI. A piece of BC hydrogel after cleaning

with NaOH solution and DI water to eliminate bacterial cells, BC aerogel obtained after freeze-drying, and the corresponding CBC after rapid plasma pyrolysis are also shown to indicate their dimensional change (Figure S1b-d). The BC aerogel has a mass of less than 1% of its hydrogel counterpart. Scanning electron microscopy (SEM) image reveals the three-dimensional web structure of BC aerogel (Figure 1b and Figure S2a), while the crosslink between nanofibers or branch structure is noted in the transmission electron microscopy (TEM) image (Figure 1c and Figure S2b).

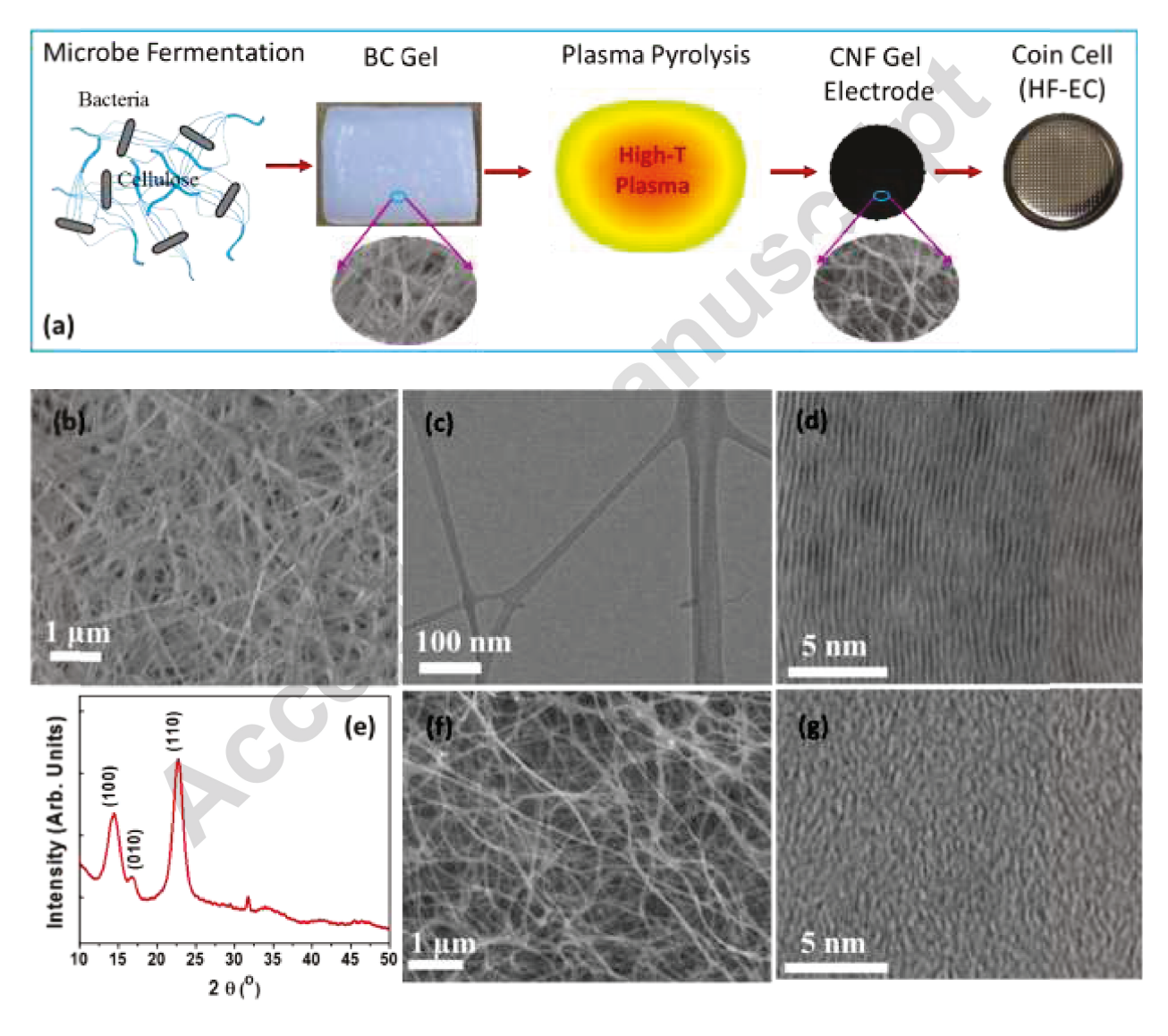


Figure 1: (a) Schematic to illustrate the whole fabrication process. (b) SEM and (c,d) TEM images of BC. (e) XRD pattern of BC. (f) SEM and (g) TEM images of CBC.

As a carbon precursor, BC is preferred over other natural celluloses due to smaller fiber size (around 10-50 nm) and higher degree of crystallinity and purity. The x-ray diffraction (XRD) pattern (Figure 1h) indicates good crystallization of the cellulose. According to the cellulose  $I_{\alpha}$  indexation, the three peaks corresponding to 20 diffraction angles of 14.45, 16.75 and 22.75 ° are indexed to (100), (010) and (110) crystallographic planes.<sup>37</sup> The high-resolution TEM image (Figure 1d) shows the (110) lattice planes with a plane spacing of 0.38 nm. Unlike individual cellulose nanofibers derived from plants that are not interconnected, the crosslinked gel structure of BC is expected to yield excellent intra-electrode conductivity after pyrolysis.<sup>34</sup> These nanoscale fibers also offer larger surface area compared to other cellulose materials composed of microscale large fibers.<sup>38-40</sup> It is interesting to note that some of the BC nanofibers exhibit a tubular-like or sheath structure (Figure S2c.e), which seems not reported previously.

Pyrolysis of polymer and cellulose precursors, including BC, to derive carbon material has been commonly conducted in a thermal process with N<sub>2</sub> or Ar environment at temperature more than 800 °C for a few to more than 10 hours.<sup>29, 31</sup> Micropore activation during this long-duration thermal process, through physical decomposition and chemical etching is also a very common practice for achieving a large surface area for electrode applications. However, as will be demonstrated, this energy-consuming thermal pyrolysis process to introduce micropores, is detrimental for the electrode frequency response, and therefore is not suitable for HF-ECs.

The concept of employing RF or microwave plasma for manufacturing carbon fibers from natural or artificial sources was developed quite long ago with a vision of scaling down the power consumption, overall cost and volume of waste chemical products. However, this technique has not been used in EC research area. In our study, BC aerogel was pyrolyzed in microwave plasma using a microwave plasma chemical vapor deposition system. We have observed that a short period (15 minutes) plasma pyrolysis of BC produced electrodes with excellent electronic conductivity, large interconnected pores for rapid electrolyte ion migration, and reasonable surface area. Without employing any further treatment, such as structural modification, doping of electrode material or applying metallic current collector that were

commonly used in other studies, the obtained CBC freestanding electrode was demonstrated to be very suitable for HF-ECs.

After plasma pyrolysis, the sample area was shrunk to about 30% and the mass was largely reduced. The morphology of CBC membrane is shown in Figure 1f and Figure S4. The overall structure is highly porous with meso- and macro-pores formed by the well-connected carbon nanofibers (CNF). The textural properties of CBC membrane were further characterized by N<sub>2</sub> sorption measurements (Figure S5). A Brunauer–Emmett–Teller (BET) surface area of 57.5 m<sup>2</sup> g<sup>-1</sup> is measured, with a pore volume of 0.374 cm<sup>3</sup> g<sup>-1</sup>. The pore size distribution shows a minimum pore diameter of 3.8 nm and the CBC is dominated by meso- and macro-pores. Without micropores, slit pores, and dead end pores, the interconnected large pores allows rapid transportation of ions in electrolyte through the electrode mesh with a low ionic resistance. Unlike a cluster simply stacked by individual CNFs or CNTs that has no intimate mechanical and electrical connection between individual fibers, well-connected CBC gel is formed by the branch structure of fibers with intrinsic connection (Figure S4c). Such a unique branched CBC web-like electrode can simultaneously offer a high ionic conductivity and a high electronic conductivity, essential for high frequency response in a 3D distributed electrode. The derived CNF is amorphous carbon (Figure 1g and S4b) without showing XRD peaks, and some of them have a tubular-like or sheath structure (Figure S4d).

#### **Aqueous cell studies**

The CBC electrodes were studied with three different thicknesses of 10, 20 and 60 um, named as CBC-10, CBC-20 and CBC-60, respectively. Their performance was evaluated in 6M KOH aqueous and 1 M TEABF<sub>4</sub> organic electrolytes. The frequency dependent behaviors were characterized via electrochemical impedance spectroscopy (EIS) measured form 100 kHz to 1 Hz, with a sinusoidal AC voltage of 10 mV amplitude, using the assembled symmetric coin cells. The methods to calculate the performance parameters can be found in the SI.

The Nyquist plot of EIS for CBC-20 based aqueous cells is presented in Figure 2a, with the zoom-in view of the high frequency region shown as the inset. A knee frequency of  $\sim 4.5$  kHz is noted. Below this frequency, the spectrum is approximately a straight line with a slope approaching 90°, and therefore the cell can be approximated by *RC* in series. Above the knee frequency, a transition region and a semicircle feature might be identified, which is ascribed to the distributed capacitance and resistance of the porous CBC electrode, a possible minor insulating layer between the coin cell package and the free-standing CBC electrode that has no extra current collector, and possibly the minor charge transfer at the electrolyte and electrode interface due to small fraction of oxygen-related remnants in CBC. These features result in a small equivalent series resistance (ESR) of 9 m $\Omega$ ·cm² in conjunction with an equivalent distributed resistance (EDR) of 26 m $\Omega$ ·cm². The Bode plot of the same EIS spectrum is presented in Figure 2b, indicating the absolute value of the phase angle generally is above 80° for frequencies up to a few hundred Hz. In particular, the cell at 120 Hz show a phase angle of  $-82^\circ$ , indicating that it maintains the capacitive nature very well at such a frequency. The characteristic frequency at  $-45^\circ$  is around 3.3 kHz.

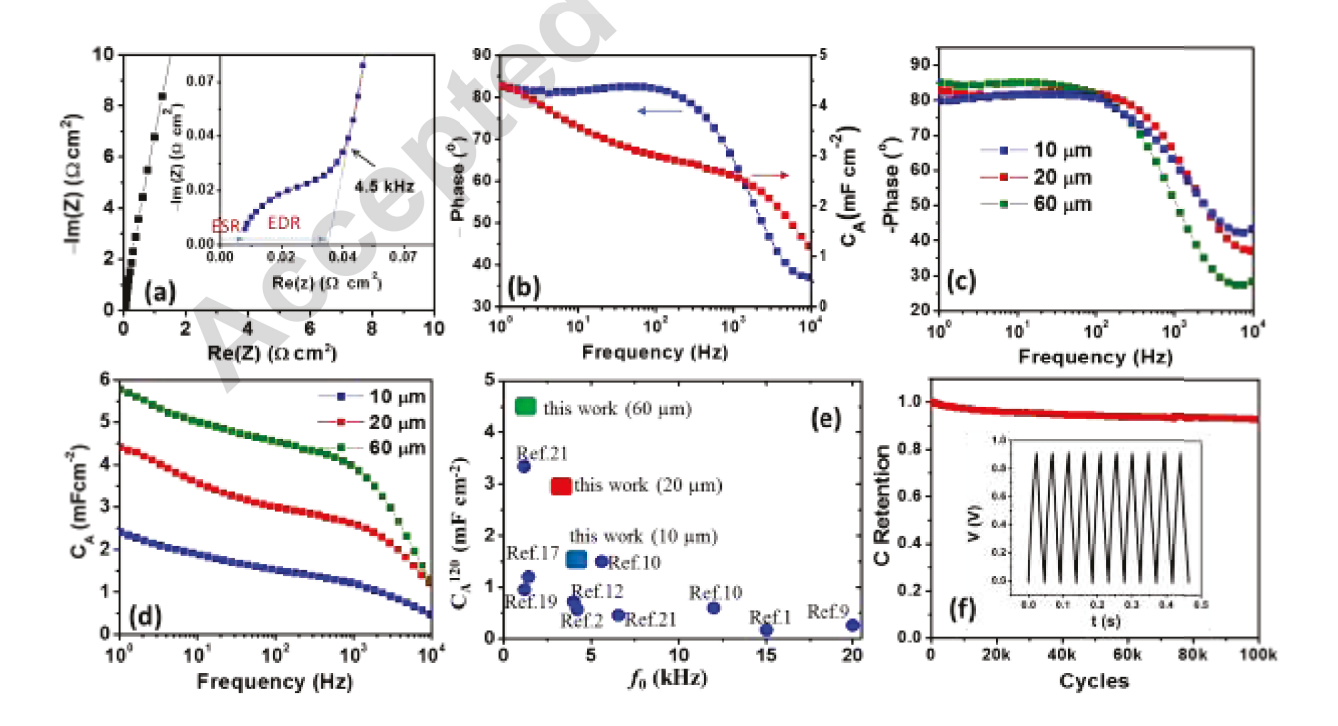


Figure 2: EIS spectra and capacitance of CBC-20 based aqueous cells: (a) Nyquist plot of the cell spectra, with the high-frequency region shown in the inset, and (b) dependence of cell phase angle and electrode capacitance on frequency. Comparison of the three electrodes in the aqueous electrolyte: (c) cell phase angle vs. frequency and (d) areal capacitance vs. frequency. (e) Performance comparison of aqueous cells in terms of the two most critical parameters for high-frequency sandwich-type cells: the electrode areal capacitance at 120 Hz and the -45° characteristic frequency. Here only selected references with  $f_0 > 1$  kHz and  $C_A^{120} > 0.2$  mF cm<sup>-2</sup> are listed. (The three squares represent data from this study for 10, 20, and 60  $\mu$ m thick electrodes, whereas blue circles are data from references.) (f) Capacitance cycling stability tested for a CBC-10 aqueous cell at 50 mA cm<sup>-2</sup>, with the inset as a section of the C-D curve.

Using the RC model, the capacitance below the knee frequency was calculated and the dependence of the areal capacitance ( $C_A$ ) of CBC-20 electrode on frequency is also shown in Figure 2b. An electrode areal capacitance as large as 2.98 mF cm<sup>-2</sup> at 120 Hz was measured. The RC time constant at 120 Hz is 0.18 ms.

The electrode thickness effect on capacitance and frequency response are presented in Figure 2c,d for the three thicknesses studied. For a frequency up to 200 Hz, they generally show a phase angle between -80° to -90°, and the characteristic frequency at -45° phase occurs at 4.1, 3.3 and 1.3 kHz for CBC-10, CBC-20 and CBC-60, respectively. In particular, the area capacitance at 120 Hz is 1.51, 2.98 and 4.50 mF cm<sup>-2</sup> for the three electrodes. It is noted that for the two thinner electrodes, the volumetric capacitance maintains a constant (~ 1.50 mF cm<sup>-3</sup>) with the areal capacitance linearly increasing. Although CBC-60 gives a very high values for areal capacitance, its volumetric counterpart (0.75 mF cm<sup>-3</sup>) falls lower compared to the thinner ones. CBC-20 offers a large areal capacitance while maintaining the volumetric efficiency. We further compare our results with those in the literature in terms of the two most critical parameters for high-frequency sandwich-type cells:  $C_A^{120}$  and  $f_0$ , with those in the literature (Figure 2e). Line-frequency AC filtering and low frequency vibration energy harvesting do not require much

higher frequency response and 1 kHz characteristic frequency might be large enough. While satisfying the frequency response requirement, our CBC electrodes exhibited extraordinary performance in terms of areal capacitance.

Cyclic voltammetry (CV) and Galvanostatic charge-discharge (C-D) cycling was further studied, as in Figure S7. Capacitance cycling stability was tested for a CBC-10 aqueous cell (Figure 2f). After 100,000 continuous cycles with full charge and discharge, the capacity was maintained at a value approximately 95% of its initial capacity. Very few studies on high-frequency ECs reported such long-cycling stability. The slight degradation of the capacitance might be related to aqueous electrolyte evaporation due to packaging.

#### Plasma pyrolysis vs. thermal pyrolysis

It is noted that several studies have employed pyrolyzed bacterial cellulose as electrodes for conventional ECs,  $^{25, 28-32}$  where typical furnace based pyrolysis and chemical activation technique was adopted. In those reports, high-density micropores and mesopores were introduced for enhanced energy density. The large electrochemical resistance arising from strong porous effect results in their sluggish frequency response, and therefore, they cannot be applied for HF-ECs. In our study, when the same BC aerogel was pyrolyzed using the conventional furnace process at  $800^{\circ}$ C for 2 hours in Ar environment, even without chemical activation, the resulting CNF film electrodes exhibited sluggish response with  $f_0$  of 8 Hz in KOH and 3Hz in TEABF4/AN organic electrolyte (Figure S8). The CBC electrodes from the long-duration thermal pyrolysis process have a very slow frequency response and are not suitable for HF-ECs.

Plasma gases also play a crucial role in determining the CBC property and its frequency response. Pure  $H_2$  plasma and  $CH_4/H_2$  (1:2) mixture plasma was both used for BC pyrolysis, and the obtained CBC has considerable different morphology and frequency response (Figure. S9). Even with the same input plasma power, the sample in pure  $H_2$  plasma had a considerable lower temperature than that in  $CH_4/H_2$  mixture plasma; the etching effect by the pure  $H_2$  plasma might also contribute to micropore generation in

CBC. Therefore, CBC pyrolyzed in  $H_2$  plasma has a characteristic frequency  $f_0 \sim 100$  Hz, more than one order of magnitude lower than in  $CH_4/H_2$  mixture plasma.

It should be emphasized that the nanoscale fibers of BC with a large surface area is a key factor for achieving large capacitance density. Microscale plant cellulose, i.e., conventional Kimwipe tissue paper, was compared with nanoscale BC. For a same thickness, the former had a capacitance  $\sim 5$  times smaller than the latter when both were prepared under the same plasma pyrolysis condition (Figure S10). All these results indicate the superiority of plasma pyrolysis of nanoscale BC crosslinked fibers for use in HF-ECs.

#### **Organic cell studies**

CBC-10, CBC-20 and CBC-60 three electrodes were also studied in 1 M TEABF<sub>4</sub> organic electrolyte. Figure 3a is the complex-plane impedance spectrum for a CBC-10 based organic cell. A knee frequency of 3.0 kHz was found, below which the spectrum can be approximated by a *RC* series model. The sum of ESR and EDR is approximately 0.33 Ω·cm², which is significantly larger than in the aqueous cell. The plot of phase vs. frequency in Figure 3b indicates a phase angle of -80° at 120 Hz. The areal capacitance vs. frequency for three electrodes are compared in Figure 3c, with a 120 Hz capacitance of 0.51, 1.08 and 2.55 mF cm<sup>-2</sup> for CBC-10, CBC-20 and CBC-60 electrodes, respectively, and the corresponding volumetric capacitances of 0.51, 0.54 and 0.425 F cm<sup>-3</sup>. The -45° characteristic frequency occurs at 1.8, 0.55 and 0.11 kHz, for CBC-10, CBC-20 and CBC-60, respectively, and the phase angles at 120 Hz are -80°, -63° and -44° (Figure S11). The ionic conductivity of electrolyte solution plays a major role in determining electrolyte dependent frequency response behavior. The ionic conductivity of TEABF<sub>4</sub> in acetonitrile solution is merely less than a hundred mS cm<sup>-1</sup>, <sup>44</sup> whereas the conductivity of TEABF<sub>4</sub> in organic solution slows the motion of the ions in the electrolyte and especially within the electrode matrix. As a result, organic cells exhibit slower response than their aqueous counterparts.

In comparison to aqueous cells, organic cells can work at much higher voltage. CV study of a CBC-10 based organic cell was performed up to 1000 V s<sup>-1</sup> rates in a potential window of 0-2.5 V (Figure 3d and Figure S12). The CV profiles maintained the desired quasi-rectangular shape even at such high rates. In fact, in TEABF<sub>4</sub>/AN organic electrolyte, the electrode may even works at a potential window up to 3.5 V (Figure 3e). This is a prominent characteristic of our organic electrolyte cells for high voltage HF-EC development. As demonstrated in Figure 3f, an organic cell was tested in 3 V window continuously for 100,000 full charge-discharge cycles. It is interesting to notice that except for initial cycles, the cell capacitance gradually increased during cycling, and it stabilized after about 50,000 cycles, with more than 20% increase of the capacitance. An increase in capacitance is expected due to complete surface area utilization. Surface wetting of nanostructured electrode depends on viscosity and surface tension of the electrolyte. Organic electrolyte has high viscosity and lower surface tension, so it typically takes longer for organic electrolyte to wet the whole active surface area, resulting the observed capacitance increase.

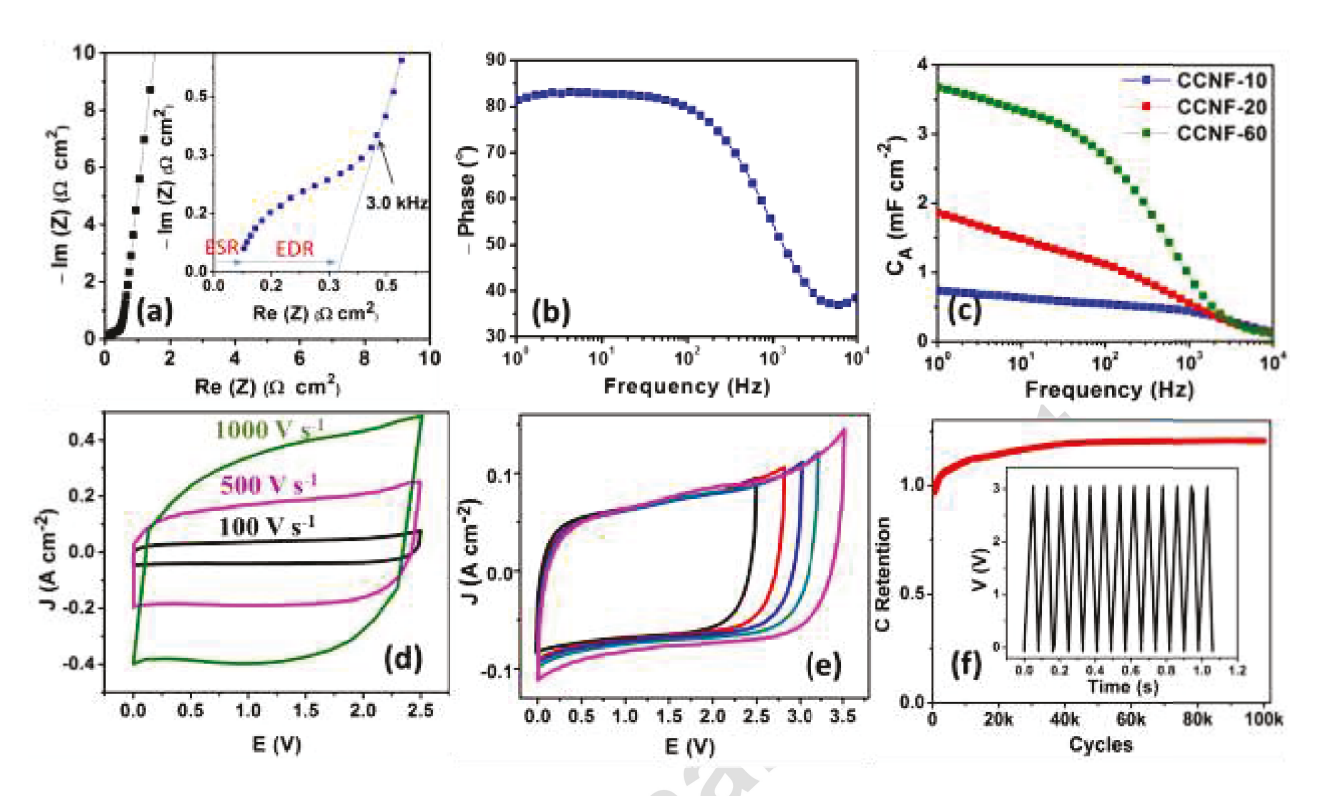


Figure 3: (a) Nyquist plot of the EIS spectra for a CBC-10 organic electrolyte cell, with the high-frequency region shown in the inset, and (b) the Bode plot of the spectrum. (c) Areal capacitance vs. frequency for the three electrodes in the organic electrolyte. (d) CV of one CBC-10 organic cell up to a rate of 1000 V s<sup>-1</sup> in a potential window 0-2.5 V. (e) CV scan at 100 V s<sup>-1</sup> in different potential windows up to 3.5 V. (f) The cell stability test up to 100K cycles with the inset as a section of C-D curve.

It was observed that the organic cells exhibit smaller capacitance than aqueous cells. The relative dielectric constant of the corresponding solvent medium certainly has a role in determining the double layer capacitance, since water has a dielectric constant of 80.1, more than double over that of acetonitrile (37.5). The difference in ionic radii of solvated ions might also impact the capacitance. The solvated ionic radii of K<sup>+</sup> and OH<sup>-</sup> are 3.31Å and 3.00 Å, respectively. In contrast, the solvated ionic radii of TEA<sup>+</sup> and BF<sub>4</sub><sup>-</sup> in acetonitrile are 13.04 Å and 11.56 Å, respectively. For larger ions, the number of

adhered ions per unit surface area will be smaller. Surface wettability (or the accessible surface area) is perhaps the most critical factor. For PECVD grown VOG electrodes, a pure carbon surface renders their hydrophobic property, and therefore a lower capacitance in aqueous electrolyte than in organic electrolyte. However, carbonized cellulose always have oxygen remains and XPS study of our CBC materials indicated ~ 5% oxygen remaining, which renders our CBC with high water absorption capability to form CBC hydrogel. These three factors result in a larger CBC electrode capacitance in aqueous electrolyte than in organic electrolyte. The capacitance difference by a few folds in aqueous and organic electrolytes was also reported previously. 46

#### **Application demonstrations**

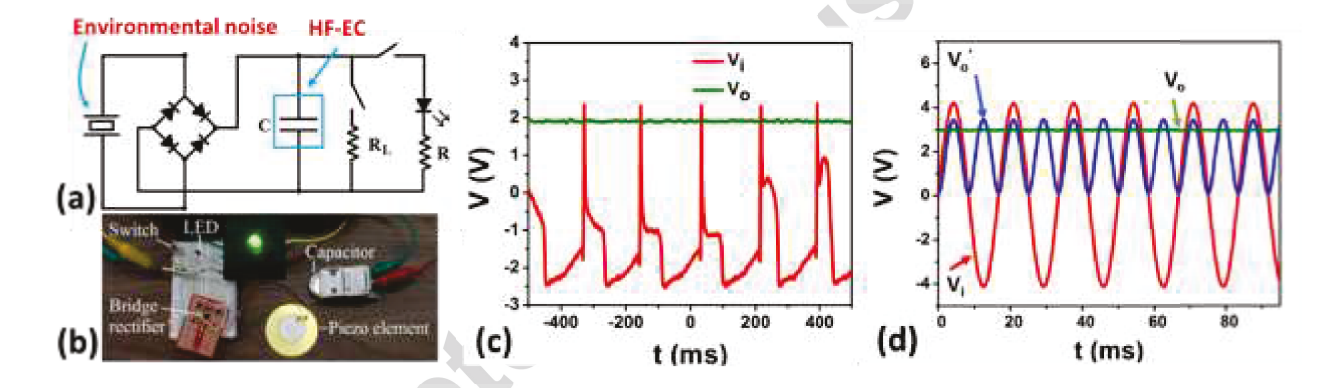


Figure 4. Demonstration of capability of HF-ECs for environmental pulse energy harvesting (a-c) and ripple current filtering (d). The schematic (a) and the photo (b) of the circuit used for pulse energy harvesting and storage. The inset photo in (b) showing that the charged HF-EC can turn on a green LED (the LED running time depends on the stored energy). (c) The irregular pulse voltage generated by the piezoelectric element under hand finger tapping  $(V_i)$  and the voltage across the HF-EC  $(V_o)$  when powering a mega ohm resistive load. (d) The input 60 Hz AC voltage wave  $(V_i)$ , the rectified pulse wave when the HF-EC was not connected  $(V_o)$  and the output DC voltage after HF-EC filtering  $(V_o)$ . A resistive load was applied for the two outputs.

To verify their potential capabilities, our CBC-10 based organic HF-ECs were used for pulse energy storage and ripple current filtering. For environmental pulse energy harvest testing, a piezoelectric element (CUI Inc. CEB-44D06) was used to generate a pulsed voltage signal from external mechanical noises. Here we used the vibration of a motor or hand finger tapping to simulate the environmental pulse energy. The testing circuit is shown in Figure 4a,b. The generated pulse from the piezoelectric element was passed through a bridge rectifier and fed across the HF-EC. A suitable Zener diode might also be used to clamp the voltage if it is over the 3V rating of the HF-EC. A 3  $M\Omega$  resistor was used to simulate a micro-power sensor load. For demonstration purpose, a green light-emitting diode (LED) was also used as a high-power pulse load. In Figure 4c, the generated electric pulses (V<sub>i</sub>) from finger tapping of the piezoelectric element is shown, and the pulse energy was stored into the HF-EC with a DC output (V<sub>o</sub>) close to 2V, which provides a constant current to the mega ohm low-power load. It can even turn on a green LED (inset of Figure 4b) for a short period. In a second experiment to simulate applications of environmental energy harvesting (Figure S13), the generated irregular pulses (V<sub>i</sub>) from a piezoelectric element, which was attached to a motor as the vibration source, were stored into an HF-EC after rectification, and the stored energy (or DC voltage V<sub>o</sub>) was supplied to power a micro-power element.

60 Hz line-frequency low-voltage AC/DC converter was also demonstrated using the circuit in Figure S14a. The AC input signal was first passed a full-wave rectifier and then filtered by a HF-EC before feeding to a load. 60 Hz sine wave with an amplitude of 4.2 V from a signal generator was applied to simulate the AC voltage in this demonstration. The input, the output after passing the full-wave rectifier when an HF-EC was not connected, and the output with the HF-EC are shown in Figure 4d and Figure S14. 3V DC voltage was obtained after the ripple voltage was smoothed by the HF-EC. These demonstrations confirm the promise of our CBC based HF-ECs for ripple current filtering and pulse energy storage.

#### Conclusion

Through a rapid plasma pyrolysis process, we demonstrated CBC aerogel is suitable as electrode for developing kHz HF-EC with extremely large areal capacitance at 120 Hz. Specifically, for 10, 20, and 60 µm thick electrodes in an aqueous electrolyte, we demonstrated their characteristic frequency at -45° phase was 4.1, 3.3, and 1.3 kHz, and the areal capacitance at 120 Hz was 1.51, 2.98 and 4.50 mF cm<sup>-2</sup>, respectively. Their voltage operation window can be further increased to ~ 3 V when an organic electrolyte used. Their excellent performance is attributed to the suitable pore size and well-crosslinked nanofiber structure of CBC aerogel that can simultaneously offer a high ionic conductivity for the electrolyte in the porous electrode, a high electronic conductivity and a large surface area, resulting in high frequency response and large areal capacitance. The potential of these kHz HF-ECs for current ripple filtering in AC/DC converter and high-frequency pulse energy storage was also demonstrated, suggesting these HF-ECs very promising for these and other similar applications.

**Acknowledgements**: This work is supported by National Science Foundation (1611060).

### Appendix A. Supplementary material

Supplementary data associated with this article can be found in the online version

#### References

- 1. Miller, J. R.; Outlaw, R. A.; Holloway, B. C., Graphene double-layer capacitor with ac line-filtering performance. *Science* **2010**, *329* (5999), 1637-9.
- 2. Sheng, K.; Sun, Y.; Li, C.; Yuan, W.; Shi, G., Ultrahigh-rate supercapacitors based on eletrochemically reduced graphene oxide for ac line-filtering. *Sci Rep* **2012**, *2*, 247.
- 3. Fan, Z.; Islam, N.; Bayne, B. S., Towards kilohertz electrochemical capacitors for filtering and pulse energy harvesting. *Nano Energy* **2017**, *39*, 306-320.
- 4. Beeby, S. P.; Tudor, M. J.; White, N., Energy harvesting vibration sources for microsystems applications. *Measurement science and technology* **2006**, *17* (12), R175.
- 5. Fan, F.-R.; Tian, Z.-Q.; Wang, Z. L., Flexible triboelectric generator. *Nano Energy* **2012**, *I* (2), 328-334.

- 6. Harne, R.; Wang, K., A review of the recent research on vibration energy harvesting via bistable systems. *Smart materials and structures* **2013**, *22* (2), 023001.
- 7. Pan, X.; Ren, G.; Hoque, M. N. F.; Bayne, S.; Zhu, K.; Fan, Z., Fast Supercapacitors Based on Graphene-Bridged V2O3/VOx Core–Shell Nanostructure Electrodes with a Power Density of 1 MW kg–1. *Advanced Materials Interfaces* **2014**, *I* (9), 1400398.
- 8. Kurra, N.; Jiang, Q.; Syed, A.; Xia, C.; Alshareef, H. N., Micro-Pseudocapacitors with Electroactive Polymer Electrodes: Toward AC-Line Filtering Applications. *ACS applied materials & interfaces* **2016**, *8* (20), 12748-12755.
- 9. Cai, M.; Outlaw, R. A.; Quinlan, R. A.; Premathilake, D.; Butler, S. M.; Miller, J. R., Fast Response, vertically oriented graphene nanosheet electric double layer capacitors synthesized from C(2)H(2). *ACS Nano* **2014**, *8* (6), 5873-82.
- 10. Ren, G.; Li, S.; Fan, Z.-X.; Hoque, M. N. F.; Fan, Z., Ultrahigh-rate supercapacitors with large capacitance based on edge oriented graphene coated carbonized cellulous paper as flexible freestanding electrodes. *Journal of Power Sources* **2016**, *325*, 152-160.
- 11. Yoo, Y.; Kim, S.; Kim, B.; Kim, W., 2.5 V compact supercapacitors based on ultrathin carbon nanotube films for AC line filtering. *J. Mater. Chem. A* **2015**, *3* (22), 11801-11806.
- 12. Ren, G.; Pan, X.; Bayne, S.; Fan, Z., Kilohertz ultrafast electrochemical supercapacitors based on perpendicularly-oriented graphene grown inside of nickel foam. *Carbon* **2014**, *71*, 94-101.
- 13. Cai, M.; Outlaw, R. A.; Butler, S. M.; Miller, J. R., A high density of vertically-oriented graphenes for use in electric double layer capacitors. *Carbon* **2012**, *50* (15), 5481-5488.
- 14. Kim, S.-K.; Kim, H. J.; Lee, J.-C.; Braun, P. V.; Park, H. S., Extremely durable, flexible supercapacitors with greatly improved performance at high temperatures. *ACS nano* **2015**, *9* (8), 8569-8577.
- 15. De Levie, R., On porous electrodes in electrolyte solutions: I. Capacitance effects. *Electrochimica Acta* **1963,** *8* (10), 751-780.
- 16. Kötz, R.; Carlen, M., Principles and applications of electrochemical capacitors. *Electrochimica acta* **2000,** *45* (15), 2483-2498.
- 17. Rangom, Y.; Tang, X. S.; Nazar, L. F., Carbon Nanotube-Based Supercapacitors with Excellent ac Line Filtering and Rate Capability via Improved Interfacial Impedance. *ACS Nano* **2015**, *9* (7), 7248-55.
- 18. Miller, J. R.; Outlaw, R. A., Vertically-oriented graphene electric double layer capacitor designs. *Journal of The Electrochemical Society* **2015**, *162* (5), A5077-A5082.
- 19. Zhou, Q.; Zhang, M.; Chen, J.; Hong, J. D.; Shi, G., Nitrogen-Doped Holey Graphene Film-Based Ultrafast Electrochemical Capacitors. *ACS Appl Mater Interfaces* **2016**, *8* (32), 20741-7.

- 20. Yoo, Y.; Kim, M. S.; Kim, J. K.; Kim, Y. S.; Kim, W., Fast-response supercapacitors with graphitic ordered mesoporous carbons and carbon nanotubes for AC line filtering. *J Mater Chem A* **2016**, *4* (14), 5062-5068.
- 21. Zhang, M.; Zhou, Q.; Chen, J.; Yu, X.; Huang, L.; Li, Y.; Li, C.; Shi, G., An ultrahigh-rate electrochemical capacitor based on solution-processed highly conductive PEDOT: PSS films for AC line-filtering. *Energy & Environmental Science* **2016**, *9* (6), 2005-2010.
- 22. Yoo, Y.; Park, J.; Kim, M.-S.; Kim, W., Development of 2.8 V Ketjen black supercapacitors with high rate capabilities for AC line filtering. *Journal of Power Sources* **2017**, *360*, 383-390.
- 23. Chi, F.; Li, C.; Zhou, Q.; Zhang, M.; Chen, J.; Yu, X.; Shi, G., Graphene-Based Organic Electrochemical Capacitors for AC Line Filtering. *Advanced Energy Materials* **2017**.
- 24. Qin, K.; Kang, J.; Li, J.; Shi, C.; Li, Y.; Qiao, Z.; Zhao, N., Free-standing porous carbon nanofiber/ultrathin graphite hybrid for flexible solid-state supercapacitors. *ACS Nano* **2015**, *9* (1), 481-7.
- 25. Chen, L.-F.; Huang, Z.-H.; Liang, H.-W.; Yao, W.-T.; Yu, Z.-Y.; Yu, S.-H., Flexible all-solid-state high-power supercapacitor fabricated with nitrogen-doped carbon nanofiber electrode material derived from bacterial cellulose. *Energy & Environmental Science* **2013**, *6* (11), 3331.
- 26. Chen, L. F.; Zhang, X. D.; Liang, H. W.; Kong, M.; Guan, Q. F.; Chen, P.; Wu, Z. Y.; Yu, S. H., Synthesis of nitrogen-doped porous carbon nanofibers as an efficient electrode material for supercapacitors. *ACS Nano* **2012**, *6* (8), 7092-102.
- 27. Pham, D. T.; Lee, T. H.; Luong, D. H.; Yao, F.; Ghosh, A.; Le, V. T.; Kim, T. H.; Li, B.; Chang, J.; Lee, Y. H., Carbon nanotube-bridged graphene 3D building blocks for ultrafast compact supercapacitors. *ACS Nano* **2015**, *9* (2), 2018-27.
- 28. Zu, G.; Shen, J.; Zou, L.; Wang, F.; Wang, X.; Zhang, Y.; Yao, X., Nanocellulose-derived highly porous carbon aerogels for supercapacitors. *Carbon* **2016**, *99*, 203-211.
- Wang, X.; Kong, D.; Zhang, Y.; Wang, B.; Li, X.; Qiu, T.; Song, Q.; Ning, J.; Song, Y.; Zhi, L., All-biomaterial supercapacitor derived from bacterial cellulose. *Nanoscale* **2016**, *8* (17), 9146-50.
- 30. Cai, J.; Niu, H.; Li, Z.; Du, Y.; Cizek, P.; Xie, Z.; Xiong, H.; Lin, T., High-Performance Supercapacitor Electrode Materials from Cellulose-Derived Carbon Nanofibers. *ACS Appl Mater Interfaces* **2015**, *7* (27), 14946-53.
- 31. Chen, L.-F.; Huang, Z.-H.; Liang, H.-W.; Gao, H.-L.; Yu, S.-H., Three-Dimensional Heteroatom-Doped Carbon Nanofiber Networks Derived from Bacterial Cellulose for Supercapacitors. *Advanced Functional Materials* **2014**, *24* (32), 5104-5111.
- 32. Kang, Y. J.; Chun, S. J.; Lee, S. S.; Kim, B. Y.; Kim, J. H.; Chung, H.; Lee, S. Y.; Kim, W., All-solid-state flexible supercapacitors fabricated with bacterial nanocellulose papers, carbon nanotubes, and triblock-copolymer ion gels. *ACS Nano* **2012**, *6* (7), 6400-6.

- 33. Wu, Z. Y.; Li, C.; Liang, H. W.; Chen, J. F.; Yu, S. H., Ultralight, flexible, and fire-resistant carbon nanofiber aerogels from bacterial cellulose. *Angewandte Chemie* **2013**, *125* (10), 2997-3001.
- 34. Li, S.; Mou, T.; Ren, G.; Warzywoda, J.; Wei, Z.; Wang, B.; Fan, Z., Gel based sulfur cathodes with a high sulfur content and large mass loading for high-performance lithium–sulfur batteries. *J Mater Chem A* **2017**, *5*, 1650-1657.
- 35. Hu, W.; Chen, S.; Yang, J.; Li, Z.; Wang, H., Functionalized bacterial cellulose derivatives and nanocomposites. *Carbohydrate polymers* **2014**, *101*, 1043-1060.
- 36. Zhu, C.; Li, F.; Zhou, X.; Lin, L.; Zhang, T., Kombucha-synthesized bacterial cellulose: Preparation, characterization, and biocompatibility evaluation. *Journal of Biomedical Materials Research Part A* **2014**, *102* (5), 1548-1557.
- 37. Castro, C.; Zuluaga, R.; Putaux, J.-L.; Caro, G.; Mondragon, I.; Ganán, P., Structural characterization of bacterial cellulose produced by Gluconacetobacter swingsii sp. from Colombian agroindustrial wastes. *Carbohydrate Polymers* **2011**, *84* (1), 96-102.
- 38. Jiang, L.; Nelson, G. W.; Kim, H.; Sim, I. N.; Han, S. O.; Foord, J. S., Cellulose-Derived Supercapacitors from the Carbonisation of Filter Paper. *ChemistryOpen* **2015**, *4* (5), 586-9.
- 39. Zhang, L.; Zhu, P.; Zhou, F.; Zeng, W.; Su, H.; Li, G.; Gao, J.; Sun, R.; Wong, C. P., Flexible Asymmetrical Solid-State Supercapacitors Based on Laboratory Filter Paper. *ACS Nano* **2016**, *10* (1), 1273-82.
- 40. Li, S.; Ren, G.; Hoque, M. N. F.; Dong, Z.; Warzywoda, J.; Fan, Z., Carbonized cellulose paper as an effective interlayer in lithium-sulfur batteries. *Applied Surface Science* **2017**, *396*, 637-643.
- 41. Paulauskas, F. L.; Yarborough, K. D.; Meek, T. T. Carbon fiber manufacturing via plasma technology. US 6372192 B1, 2002.
- 42. Ren, G.; Hoque, M. N. F.; Liu, J.; Warzywoda, J.; Fan, Z., Perpendicular edge oriented graphene foam supporting orthogonal TiO 2 (B) nanosheets as freestanding electrode for lithium ion battery. *Nano Energy* **2016**, *21*, 162-171.
- 43. Gilliam, R. J.; Graydon, J. W.; Kirk, D. W.; Thorpe, S. J., A review of specific conductivities of potassium hydroxide solutions for various concentrations and temperatures. *International Journal of Hydrogen Energy* **2007**, *32* (3), 359-364.
- 44. Béguin, F.; Presser, V.; Balducci, A.; Frackowiak, E., Carbons and Electrolytes for Advanced Supercapacitors. *Advanced Materials* **2014**, *26* (14), 2219-2251.
- 45. Zhong, C.; Deng, Y.; Hu, W.; Qiao, J.; Zhang, L.; Zhang, J., A review of electrolyte materials and compositions for electrochemical supercapacitors. *Chemical Society Reviews* **2015**, *44* (21), 7484-7539.

46. Kim, Y.-J.; Masutzawa, Y.; Ozaki, S.; Endo, M.; Dresselhaus, M. S., PVDC-based carbon material by chemical activation and its application to nonaqueous EDLC. *Journal of The Electrochemical Society* **2004**, *151* (6), E199-E205.





Ms. Nazifah Islam is a Ph.D. student in the Department of Electrical and Computer Engineering at Texas Tech University under supervision of Prof. Zhaoyang Fan. She completed her Bachelor degree from Bangladesh University of Engineering and Technology. Her research interest includes studies of nanostructured materials for energy conversion and storage devices. She is currently working on development of electrode material and design towards compact high-frequency supercapacitors.



Dr. Shiqi Li received his B.S. degree from Wuhan University in 2005 and Ph.D. from Peking University in 2010. After several years in the industry and in the academy, he was appointed as an associate professor at Hangzhou Dianzi University in 2017. His interest focuses on electrochemical energy storage, particularly Li-S battery, Li metal anode, and supercapacitors.



Dr. Guofeng Ren received his Ph. D. degree from Texas Tech University in 2016. Before that he earned his Bachelor degree from Lanzhou University in 2010. Currently he is a research associate at Case Western Reserve University. His research interests include lithium ion batteries, lithium sulfur batteries and solid state batteries.



Yujiao Zu received her B.S. in Engineering of Microbiology and then her M.S. in Food Science form Tianjin University of Science and Technology of China. She is a third year doctoral student in the department of Nutritional Sciences at Texas Tech University. Her research interest is Nanomedicine. She is currently working on targeted delivery of resveratrol to adipose tissues to prevent and treat obesity.



Dr. Juliusz Warzywoda received his Ph.D. degree in Chemical Engineering from Worcester Polytechnic Institute (WPI) in 1989. He currently oversees the operation of Materials Characterization Center at Texas Tech University. Prior to joining Texas Tech, he was a senior research scientist at the NASA-sponsored Center for Advanced Microgravity Materials Processing at Northeastern University. He has worked on the synthesis and characterization of zeolites and related materials for use as (photo)catalysts and in optoelectronics; microporous thin film synthesis/preparation; experimental and theoretical aspects of zeolite/zeotype nucleation and crystal growth; and materials processing in microgravity.



Dr. Shu Wang received her medical degree from Jilin University in China, her master's in biochemistry and molecular biology from Capital Medical University in China, and her Ph.D. in nutritional biochemistry and metabolism from Tufts University in Massachusetts in USA. Dr. Shu Wang is an associate professor in the Department of Nutritional Sciences at Texas Tech University. Her research focuses on using biocompatible and biodegradable nanocarriers to enhance bioactivities of phytochemicals for the prevention and treatment of chronic diseases.



Dr. Zhaoyang Fan Obtained his B.E and M.E degrees from Tsinghua University of China and Ph.D. from Northwestern University of U.S. He is an associate professor in Department of Electrical and Computer Engineering and Nano Tech Center, Texas Tech University. His research concerns synthesis and property study of nanomaterials and semiconductors, and their applications for photonics and clean energy.

#### Highlights

- Through microbe fermentation process, cellulose nanofiber aerogel was synthesized
- Rapid plasma pyrolysis of cellulose aerogel into carbon nanofiber aerogel was investigated
- KHz high-frequency ECs with electrode capacitance as high as 4.5 mF cm<sup>-2</sup> at 120 Hz.
- KHz ECs operates at 3V were demonstrated.
- ed t KHz ECs for pulse energy storage in energy harvesting were demonstrated for the first time.

#### **TOC** graphic

Through microbe fermentation process, cellulose nanofiber aerogel was synthesized, which was converted to crosslinked carbon nanofiber aerogel in a rapid plasma pyrolysis process. Using such highly conductive carbon aerogel with large surface area and tailed porous structure, kilohertz high-frequency electrochemical capacitors (HF-EC) with large areal capacitance as high as 4.5 mF cm<sup>-2</sup> at 120 Hz were demonstrated. HF-ECs operated at 3V were further demonstrated for pulse energy storage in environmental noise energy harvesting system for the first time.

